Fouling of nanofiltration membranes based on polyelectrolyte multilayers: The effect of a zwitterionic final layer

Ettore Virga [a,b], Klara Žvab [b], Wiebe M. de Vos [a,*]

[a] Membrane Science and Technology, University of Twente, Drienerlolaan 5, 7522, NB, Enschede, the Netherlands
[b] Wetsus, European Centre of Excellence for Sustainable Water Technology, Oostergoweg 9, 8911, MA, Leeuwarden, the Netherlands

ARTICLE INFO

ABSTRACT

In this work, we investigate the effect of membrane surface chemistry on fouling in surface water treatment for polyelectrolyte multilayer based nanofiltration (NF) membranes. The polyelectrolyte multilayer approach allows us to prepare three membranes with the same active separation layer, apart from a difference in surface chemistry: nearly uncharged crosslinked Poly(allylamine hydrochloride) (PAH), strongly negative poly(sodium 4-styrene sulfonate) PSS and zwitterionic poly(2-methacryloyloxyethyl phosphorylcholine-*co*-acrylic acid) (PMPC-*co*-AA). Initially, we study foulant adsorption for the three different surfaces (on model interfaces), to demonstrate how a different surface chemistry of the top layer affects the subsequent adsorption of five different model foulants (Humic Acids, Alginates, Silica Nanoparticles, negatively and positively charged Proteins). Subsequently, we study fouling of the same model foulants on our polyelectrolyte multilayer based hollow fiber NF membranes with identical surface chemistry to the model surfaces. Our results show that nearly uncharged crosslinked PAH surface generally fouls more than strongly negatively charged PSS surface. While negative BSA adsorbs better on PSS, probably due to charge regulation. Overall, fouling was mainly driven by electrostatic and acid-base interactions, which led, for both PAH and PSS terminated membranes, to flux decline and changes in selectivity. In contrast, we demonstrate through filtration experiments carried out with synthetic and real surface water, that the bio-inspired zwitterionic phosphatidylcholine surface chemistry exhibits excellent fouling resistance and thus stable performance during filtration.

1. Introduction

High quality drinking water is produced worldwide from surface water. This is partly possible thanks to the advances made in membrane filtration. In the last 20 years, membrane filtration has started to replace conventional water treatment techniques, such as coagulation, flocculation, sedimentation, flotation, and sand filtration [1,2]. This is especially due to their versatility: membranes allow the removal of a wide spectrum of components, ranging from suspended solids (microfiltration) to small organic pollutants and ions (reverse osmosis) [2].

Among the various filtration techniques, nanofiltration (NF) has become an increasingly established technology in surface water treatment [3]. NF allows the removal of humic substances [4,5], micropollutants [6,7], heavy metals and salinity [8] from surface water, with a substantially lower energy footprint than reverse osmosis [2,9].

However, one of the main challenges of membrane filtration is fouling [3,10]. Membrane fouling is influenced by physical (e.g. permeation drag, shear forces) and chemical factors (e.g. hydrophobic interactions, ions binding effects) [11]. Humic acids, proteins, polysaccharides and solid particles can adsorb at the membrane surface and inside pores, and consequently reduce the flux of treated water. This phenomena leads to an increase in operating costs [10] and the need for membrane chemical cleaning [12], which in turn compromises the membrane stability over time [13]. Moreover, the presence of a fouling layer can have substantial impact on the membrane separation properties [14–16], especially on the retention of charged solutes, by changing the membrane surface charge density [17]. For NF, fouling can even be more complex to investigate, since the interactions that lead to fouling take place at the nanoscale, both in an on the active separation layer [3, 18].

Membrane surface chemistry plays a crucial role in fouling [19,20]. Membrane fouling is a phenomena that occurs at the water-membrane interface, where foulants-surface interaction takes place [21,22]. Membrane surface properties, such as surface charge, chemistry and

---

* Corresponding author.
  E-mail address: w.m.devos@utwente.nl (W.M. de Vos).

roughness thus become very important [23]. A much investigated approach to reduce membrane fouling is to minimize the attractive interactions between the surface of the membrane and the foulants contained in the feed [24,25]. For this reason, surface modification of existing membranes is considered an effective tool to reduce foulant-membrane interactions and indeed to design low fouling membranes [26–28].

An easy way to control the membrane surface chemistry and at the same time its separation properties, is the so called Layer-by-Layer (LbL) technique [29–32]. In LbL, a charged membrane is coated alternately with positive and negative polyelectrolytes, which overcharge the surface of the membrane during every coating step [33]. LbL allows a great deal of control over the properties of the active separation layer, while at the same time it provides large freedom on the choice of membrane surface chemistry [34–36]. This easy technique is proven to increase ion retention [37], selectivity [38,39], and additionally to reduce membrane fouling [28,40–42], but it typically leads to a surface with an excess of positive or negative charge [43].

The charge of the membrane surface is a key parameter in the design of low fouling membranes. Since several colloidal materials have a slight negative charge, due to the presence of acid groups (e.g. carboxyl, sulfonic and hydroxil), most commercial membranes are designed with a negative surface charge to reduce fouling [44]. Hydrophilic and negative membranes are less prone to fouling than positive ones, but a zwitterionic chemistry can further enhance membrane low-fouling properties [45–47]. Recently, among a new class of high-flux and fouling resistant zwitterionic-based membranes [48], the effect of different zwitterionic chemistries was investigated, and membranes prepared with 2-methacryloyloxyethyl phosphorylcholine (MPC) showed unprecedented fouling resistance during the filtration of proteins [49].

In this work, we investigate the effect of membrane surface chemistry on fouling in surface water treatment for polyelectrolyte multilayer based nanofiltration membranes. Polyelectrolyte multilayers are ideal for such as study, as it is easy to create identical separation layers, with just the final layer having a different surface chemistry. Moreover, these membranes provide highly promising separation properties and thus very relevant membranes. Initially, the focus is on foulant adsorption on polyelectrolyte multilayers prepared on model surfaces to demonstrate how a different surface chemistry of the top layer (nearly uncharged crosslinked Poly(allylamine hydrochloride) (PAH), strongly negative poly(sodium 4-styrene sulfonate) PSS and zwitterionic poly(2-methacryloyloxyethyl phosphorylcholine-*co*-acrylic acid) (PMPC-*co*-AA)) affects the subsequent adsorption of five different model foulants (Humic Acids, Alginates, Silica Nanoparticles, negatively and positively charged Proteins). Subsequently, we study fouling of the same model foulants on our PEM based hollow fiber NF membranes with identical

surface chemistry to the model surfaces (Fig. 1). Through filtration experiments carried out with synthetic and real surface water, we demonstrate that especially the zwitterionic surface chemistry, bioinspired by zwitterionic phosphatidylcholine (PC) headgroups located on cell membranes, exhibits a very low susceptibility to fouling and leads to stable membrane performance.

2. Materials and methods

2.1. Chemicals

Poly(allylamine hydrochloride) (PAH, Mw = 50 kDa), poly(sodium 4-styrene sulfonate) (PSS, Mw = 70 kDa), an aqueous solution of 25 wt% glutaraldehyde (GA, Grade II), acrylic acid (AA), 2-methacryloyloxyethyl phosphorylcholine (MPC, 295.27 Da), *N*-(3-Dimethylaminopropyl)-*N*-ethylcarbodiimide hydrochloride (EDC), *N*-Hydroxysuccinimide (NHS), ammonium persulfate ($(NH_4)_2S_2O_8$) and glycerin were purchased from Sigma-Aldrich (The Netherlands). Our model foulants, Alginic acid sodium salt from brown algae (Sodium alginate), Bovine Serum Albumin (BSA, chromatographically purified, $\geq$ 98%), LUDOX® (AS-30 colloidal silica 30 wt% suspension in H_2O) and Lysozyme (from chicken egg white powder, crystalline 70,000 U/mg), were purchased from Sigma-Aldrich (The Netherlands), whereas humic acids (Suwannee River Humic Acid Standard III) were purchased from International Humic Substances Society. Anthracite (1.2–2.0 mm) and sand (0.5–1.0 mm), used in the pre-filtration step, were supplied by SIBELCO Filcom B.V. (The Netherlands). A cartridge filter (DGD-2501 Dual-Gradient Polypropylene 25/1 20) was supplied by Pentair (The Netherlands). All other chemicals were purchased from VWR (The Netherlands).

2.2. Zwitterionic copolymer synthesis

Even if PMPC-co-AA is not purely zwitterionic [50] (due to the presence of AA groups), in the text we refer to it as zwitterionic. AA was added to the polymer to give a charge excess, needed to build-up the multilayer [51,52], and allow for chemical crosslinking (via EDC and NHS) to the multilayer.

Our recipe for the synthesis of the zwitterionic PMPC-co-AA copolymer, was adapted from a recipe used for the synthesis of PSBMA [53]. 100 mL of demi water was flushed with nitrogen for 1 h in a 500 mL Duran® bottle. In this, 5.0 g (16.8 mmol) MPC was dissolved under nitrogen atmosphere and later 2.42 g (33.6 mmol) AA was added. After 1 min, 0.228 g (1 mmol) $(NH_4)_2S_2O_8$ was added. The mixture was left to react under nitrogen atmosphere at room temperature for 23 h and then heated up to 50 °C and left reacting for 2 h more. Finally, the mixture was cooled down to room temperature and mixed with 400 mL of
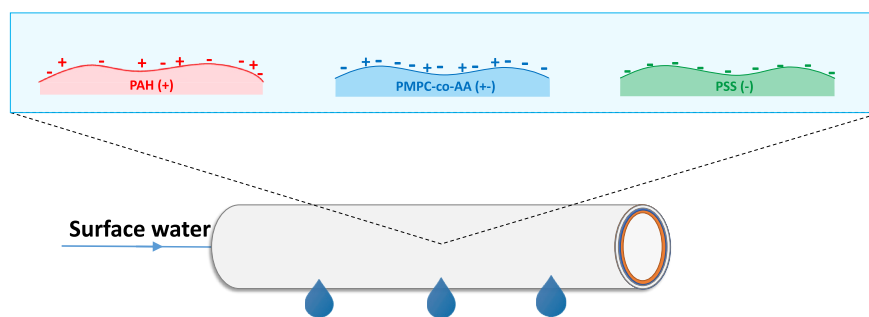

Fig. 1. Illustration of a hollow fiber membrane with the same multilayer, except from the final adsorbed layer that determines the membrane surface chemistry.

Ethanol to precipitate the polymer. The precipitated polymer was washed three times with 50 mL acetone and subsequently dried in a vacuum oven for 2 days. The zwitterionic copolymer was stored under vacuum to prevent water uptake and was used without any purification steps. Using ^{1}H NMR, the monomer distribution was estimated to be approximately 1:2 mol ratio of MPC/acrylic acid (see Fig. S1, Supporting Information, SI, for further details). This ratio allows for an adequate polymer charge excess, making the build-up of the multilayer easier.

2.3. Model surfaces coating with PEM

Polyelectrolyte solutions were prepared to have a concentration of 0.1 g/L polyelectrolyte dissolved in a 50 mM NaCl solution without pH adjustment (pH ~ 5.5). Each coating step was performed at room temperature. First, negatively charged SiO_2 wafers were cleaned with piranha solution to remove possible contaminants. Subsequently, the wafers were dipped for 15 min in a polycation (PAH in 50 mM NaCl) solution and then rinsed with a 50 mM NaCl aqueous solution for at least 15 min to remove any polyelectrolyte not well attached to the surface. To complete the first bilayer, the wafers were then immersed in polyanion (PSS in 50 mM NaCl) solution for 15 min. This step was then followed by another rinsing step. The procedure was repeated until the desired number of bilayers was reached. We coated 4.5 bilayers for the nearly uncharged (PAH) terminating layer, 5 bilayers for the negative (PSS) terminating layer. For the zwitterionic top layer, PMPC-co-AA was coated on top of 4.5 bilayers made of PAH/PSS. In addition, the model surfaces were crosslinked to improve their stability. In case of PAH and PSS as top layers, the surfaces were immersed in a 7.5 mM glutaraldehyde for 5 h, as described in our previous work [54], while in case of zwitterionic top layer, the wafers were firstly immersed in a 5 mM NHS and a 25 mM EDC solution for 1 h to crosslink just the top layer [55,56] and later in a 7.5 mM glutaraldehyde for 5 h. We apply the same coating procedure on membranes (see paragraph 2.5).

2.4. Fouling study on model surfaces via reflectometry

Several compounds are present in typical surface water, including proteins, polysaccharides, humic acids, extracellular polymeric substances and solid particles. These fouling agents tend to adsorb on membrane surfaces and form a gel layer which can significantly promote bacterial growth and cause significant reduction in the flux of treated water [57]. For such a mixture of compounds, fouling can be difficult to study. Here, we have chosen to study five model compounds: negatively and positively charged proteins (i.e. BSA and Lysozyme), Humic Acids from Suwannee River, Alginates from brown algae, and LUDOX® colloidal silica.

We first studied fouling by the five foulants on model surfaces using reflectometry as investigation tool [58]. In order to determine the quantity of fouling agent adsorbed at the surface, we flushed different fouling agents in artificial surface water (with composition 2.92 mM NaCl, 0.57 mM $MgSO_4$, 1.47 mM $CaSO_4$ and 0.3 mM $MgCl_2$, paragraph 2.6) to silica surfaces, previously dip-coated with PEM as described above. After steady state in adsorption is reached, the surfaces rinsed with the same solution without fouling agents. The foulant adsorption/desorption here occurs under well control hydrodynamic conditions, thanks to the use of a stagnation point flow cell. A polarized monochromatic light (HeNe laser, 632.8 nm), after hitting the wafer around the Brewster angle, is reflected towards a detector and splits into two polarized components. S (−) is the ratio between the two polarized components, and ΔS the change in this ratio, used calculate the mass of foulant adsorbed or desorbed from the model surface

$$\Gamma = \frac{\Delta S}{S_0} Q. \tag{1}$$

where Γ is the quantity of foulant (mg/m^{2}) which adsorbs or desorbs

from the model surface, S_0 is the initial output signal of the model surface (−), and Q is the sensitivity factor (mg/m^{2}). To calculate Q, we used an optical model based on the following values: $\theta = 71°$, $n_{Si} = 1.46$, $\tilde{n}_{SiO_2} = (3.85; 0.02)$, $n_{H_2O} = 1.33$, $\delta_{SiO_2} = 90nm$ and refractive index increment dn/dc (mL/g), shown in Table 1. The calculated sensitivity factors Q for all fouling agents are also shown in Table 1. All experiments were performed at least in duplicate.

2.5. Hollow fiber membranes coating

Polyelectrolyte multilayers were coated on sulfonated polysulfone (SPES) hollow fiber membranes with a water permeability of 150 LMH/bar, an inner diameter of 0.7 mm, and a molecular weight cutoff (MWCO) of 7.5 kDa [54]. First, the fibers, stored in fresh water, were immersed in a 50 mM NaCl solution for 2 min at room temperature. Second, the fibers were fully dipped in a 0.1 g/L PAH solution with 50 mM NaCl for 15 min. Later, a rinsing step with a 50 mM NaCl solution followed and, after 15 min, the fibers were immersed in 0.1 g/L PSS solution with 50 mM NaCl (15 min) followed by another rinsing step (50 mM NaCl, 15 min). The described dip coating procedure was repeated until the desired number of bilayers was reached. In the case of PAH and PSS terminated layers, the fibers were crosslinked by immersion in a 7.5 mM GA solution for 5 h. In the case of zwitterionic terminated layer, the fibers were first immersed in a 5 mM NHS and 25 mM EDC solution for 1 h, and then dipped in a 7.5 mM glutaraldehyde solution with 50 mM NaCl for 5 h. After rinsing in demi-water, the membranes were immersed in a solution of glycerol and water (15/85 wt %) for 4 h and left drying overnight at room temperature. Later, each single fiber, coated with PEM, was potted in a module with a fiber length of approximately 170 mm and mounted in our crossflow experimental set-up (Fig. S2 and Figs. S3 and SI), were tested in order to measure water permeability and ion retention. We calculated the water permeability (LMH/bar, Fig. S4) as ratio between the pure water flux and the transmembrane pressure (TMP). Fluxes were measured at room temperature using demi-water at a transmembrane pressure of 3 bar. In order to measure the salt retention, we analyzed the ionic content of the feed and permeate by using ion chromatography (Metrohm Compact IC 761). All experiments were performed at least in triplicate.

2.6. Filtration of artificial surface water

In order to investigate the role of the chemistry of the final layer on membrane fouling, we prepared fouling solutions with a 100 mg/L concentration of fouling agent and pH = 6.3–6.5. We dissolved our fouling agents (sodium alginate, BSA, lysozyme, humic acid and LUDOX®, paragraph 2.4) in artificial surface water with the following composition: 2.92 mM NaCl, 0.57 mM $MgSO_4$, 1.47 mM $CaSO_4$ and 0.3 mM $MgCl_2$. This composition reflects the composition of the natural surface water (IJsselmeer, Afsluitdijk, The Netherlands) [62] used in our experiments with real river water (paragraph 2.7). In order to simplify the study, carbonate salts were not added to the artificial surface water. For the membrane crossflow filtration experiments, we use modules with single PEM-coated fibers as described in paragraph 2.5. The clean water flux and ions retention of every fiber was measured before filtration of the fouling agent. We used new modules for each different

Table 1
Reflective index increments (dn/dc) and sensitivity factors for the fouling agents.

Fouling agent	dn/dc (mL/g)	Q (mg/m^{2})
Lysozyme	0.19 [59]	30
BSA	1.67 [59]	30
Sodium alginate	0.165 [59]	30
LUDOX®	0.06 [60]	90
Humic acids	0.28 [61]	20

set of experiments. We recycled the concentrate stream to the feed tank while we collecting the permeate for 1 h. We checked the pH, ionic concentration and TOC of the feed at every start and end of each experiment, to ensure that no significant changes in feed composition occurred, for example due to the used re-cycle. Such changes were never observed.

During the membrane filtration experiments a fouling solution was filtered for 3 h at a TMP of 3 bar and a flow-rate of 0.75 kg/h (crossflow velocity 0.55 cm/s, Reynolds number ~380). We measured the permeate flux between 2 h and 3 h after the start of the experiment. We collected permeate samples and analyzed their ionic concentration and TOC by ion chromatography (Metrohm Compact IC 761) and a TOC analyzer (Shimadzu TOC-L), respectively. Feed samples were taken before and after each experiment. To clean the membranes, the modules were exposed for 15 min to artificial river water at a 3.75 kg/h flow-rate, without applying TMP. Finally, we measured again the water permeability to calculate the flux recovery. Each experiment was performed at least in triplicate.

2.7. Real surface water filtration

Surface water was collected at the IJsselmeer (Afsluitdijk, The Netherlands) and pre-filtered, first, with a sand filter and, second, with a cartridge filter, in order to remove bigger particles and bacteria, which are not relevant for this study. The sand filter used in the pre-filtration step is based on two medias: anthracite (1.2–2.0 mm) and sand (0.5–1.0 mm). Each media has a 50 cm height. After the sand filter, a microfiltration step based on cartridge filter (1–25 μm) was applied to the water stream. The filtered surface water was later stored at 5°C and analyzed before each experiment. Its composition is reported in the Table 2.

For the membrane crossflow filtration experiments, we use modules with single PEM-coated fibers as described previously (paragraph 2.5). The clean water flux of every fiber was measured before the filtration of surface water. New modules were used for each different set of experiments. We recycled the concentrate to the feed tank and discharged the permeate, on the time scale of the experiment this did not lead to changes in the feed composition. Those small changes were measured and took into account by analyzing the feed pH, ionic content and TOC at the start and end of each experiments, by using average values in the retention calculations. During the membrane filtration experiments the surface water was filtered for 20 h, again, at a TMP of 3 bar and a flow-rate of 0.75 kg/h (crossflow velocity ~0.55 cm/s, Reynolds number ~380). We measured again the permeate flux after 20 h experiment. We collected permeate samples and analyzed their ionic concentration as discussed above. To clean the membranes, the modules were exposed to DI water for 15 min at a 3.75 kg/h flow-rate, without applying transmembrane pressure. Finally, we measured again the water permeability to calculate the flux recovery. Each experiment was performed at least in triplicate.

Table 2

Composition of the pre-filtered surface water (IJsselmeer, Afsluitdijk, The Netherlands), feed water of the membrane crossflow experiments.

	Concentration (mg/L)
Ca^{2+}	52.8 ± 3.2
Na^+	81.7 ± 2.8
Mg^{2+}	15 ± 0.6
SO_4^{2-}	68.4 ± 2.6
Cl^-	136 ± 5.3
TOC	8.4 ± 1.6

3. Results and discussion

This Section is split into three distinct main parts. In the first part, we study the adsorption of model foulants, such as bioproteins (Lysozyme and BSA), standard humic acids, silica nanoparticles (LUDOX®) and alginates, on PEMs prepared on model surfaces with final layers with different charge and surface chemistry. In the second part, we investigate fouling by the same model foulants on hollow fiber membranes coated with identical polyelectrolyte multilayers. Here we investigate how the three different membrane top layers affects fouling in NF and additionally. In the third part, we apply our membranes for real surface water treatment, and analyze our previous results in terms of overall membrane performance and stability.

3.1. Foulant adsorption on model surfaces

During membrane operation, the chemistry of the foulants and the membrane surface are key parameters that will determine the extend of adsorption at the membrane surface. Using optical reflectometry, we studied the foulant adsorption on model surfaces pre-coated coated with same PEM, $(PAH/PSS)_{4.5}$, but with different surface chemistries of the final top layer. Each PEM was exposed to a fouling solution until a steady state in foulant adsorption was reached. The steady state in adsorption corresponds to the total amount of foulant adsorbed on the multilayer. In order to determine the amount of irreversible and reversible adsorption for every single fouling agent, the wafer was later flushed with a rinsing solution with the same pH and ion concentration as the fouling solution. This procedure allows to neglect possible effects on the optical signal due to changes in surface zeta potential and ion binding [63–65]. The irreversibility of foulant adsorption on model surfaces is discussed in the Supporting Information (SI).

In Fig. 2 we show the adsorption of the five model foulants, previously described, on $(PAH/PSS)_{4.5}$ based PEM with three different top layers: nearly uncharged crosslinked PAH, negatively charged PSS and zwitterionic PMPC-co-AA.

The absolute adsorption values are generally small when compared with other results from literature. While Lysozyme adsorption was found to be ~0.9 mg/m^2 and 0.7 mg/m^2, respectively for bare and polystyrene-coated silica surfaces [66,67], for all the other foulants higher adsorption values are normally reported in literature. BSA adsorption was found to be ~10 and 25 mg/m^2, respectively for negatively charged PAA brushes [68] and positively charged PAH terminated multilayers [69]. Also, LUDOX®, Alginate and HA are well known for giving high adsorbed amounts (>6 mg/m2) especially on positive or neutral surfaces [69–72]

PEMs allow for highly hydrophilic and smooth surfaces [40,41] which are well known to be less prone to foul [23,73,74]. Even if the adsorption values for all the foulants are relatively small, from Fig. 2 we do observe that electrostatic interactions play a crucial role in foulant adsorption. Negatively charged foulants such as LUDOX®, Alginate and HA adsorb more on nearly uncharged crosslinked PAH (Fig. 2A), in comparison to the negatively charged PSS (Fig. 2B). On the other side, positively charged foulants, such as lysozyme, adsorb more on negatively charged PSS top layers.

However, adsorption is not only driven by charge based interactions between top layer and foulant, but Lewis acid-base interactions could also play a crucial role [75]. In Lewis acid-base interactions unpaired electrons are shared among polar surface functional groups (e.g membrane moieties), water molecules, and polar functional groups on the opposing surface or molecule (e.g. foulant) [76].

Negatively charged BSA adsorbs more on the negative PSS top layer (see Fig. 2B), while negative LUDOX® nanoparticles lead to high adsorbed amounts on the zwitterionic PMPC-co-AA (see Fig. 2C). BSA may adsorb better on negatively charged PSS due to charge regulation, an effect that can lead to a charge inversion of the protein [68]. In addition, this adsorption may also be driven by the fact that BSA is a
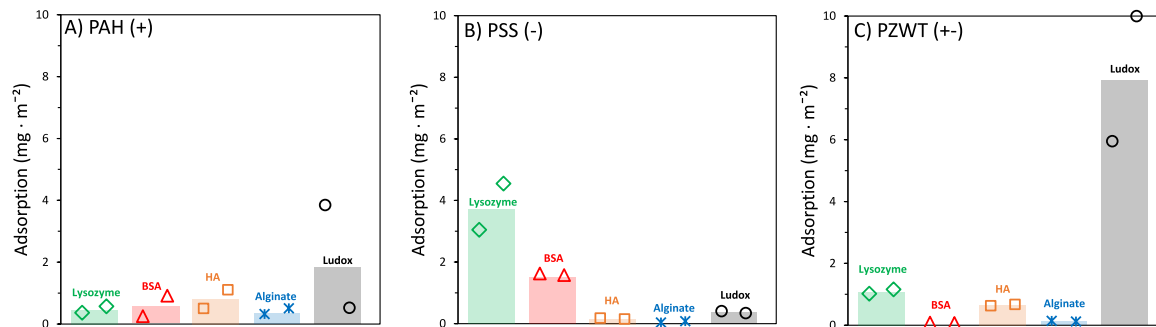
Fig. 2. Adsorption (mg/m^2) of model fouling agents on model surfaces coated with PAH (A), PSS (B) and PMPC-co-AA (C) top layers. Results obtained via reflectometry. Bars show average values, while markers show data points from all individual measurements.

patchy protein, having at pH = 6.5 a small region that is positively charged [77]. This region of the protein could complex with the negatively charged PSS [33]. On the other side, LUDOX® nanoparticles may adsorb better on the zwitterionic PMPC-co-AA probably due to hydrogen bond formation between the polymer phosphorylcholine groups and silica hydroxyls [78].

Adsorption is only an indication of how prone a surface is to fouling. Adsorption is not the only mechanism for membrane fouling, but usually foulant-foulant interactions dominate [79]. These interactions, and the constant accumulation of fouling agents at the membrane surface due to permeation, are responsible for the build-up of a cake layer [79,80].

3.2. Effect of foulant chemistry on membrane fouling

The rejection of charged species, such as cations, anions or charged organic molecules, can change due to membrane fouling. During filtration, foulants can adsorb at the membrane surface and pores, changing the original surface chemistry of the membrane. Therefore, fouling could lead to a decrease in water permeability as well as a change in ion and organics retentions, as a consequence of the change in membrane surface chemistry.

In order to monitor fouling for the three different top layers during filtration, first we measure the flux decline of our membranes with pure water and later perform a 3 h experiment with synthetic surface water containing one of the model foulants. Then, we define as flux decline the ratio between the flux during model foulant filtration and the previously measured flux of pure water. Here, we also measure the ion retentions of clean and fouled membranes, since it helps us in understanding if the surface chemistry of our membrane changed due to the build up of a

fouling layer. We finally try to quantify the membrane flux recovery by first flushing the membrane with synthetic surface water without any fouling agent and then measuring again the flux of pure water. We applied this method to all fouling agents: Lysozyme, BSA, LUDOX®, Alginate and HA.

3.2.1. Ion retentions for clean membranes

In Fig. 3, we show ion retentions for clean hollow fiber membranes when synthetic surface water (without addition of foulants) is used. Fig. 3A, B and 3C respectively show ion retentions for nearly uncharged crosslinked PAH, negatively charged PSS and zwitterionic PMPC-co-AA top layers. In particular, we show retentions of Ca^{2+}, Na^+, Mg^{2+}, SO_4^{2-} and Cl^-. For each top layer, we can see that the rejection of ions is probably determined by both Donnan and dielectric exclusion [81]. We show high rejection of sulphate ions, in particular for anionic PSS (Fig. 3B) and zwitterionic PMPC-co-AA (Fig. 3C) top layers. All the membranes investigated have a negative zeta potential. In particular, the zeta potentials for PAH, PSS and PMPC-co-AA top layers are respectively −11.8, −37.4 and −24.7 mV (SI, Fig. S5). Crosslinking of the weakly cationic primary amines of PAH changes the charge balance in the multilayer, decreasing the positive charge leading to a small negative surface charge [82]. This leads to a stronger Donnan-based repulsion towards SO_4^{2-}, as already shown in previous works [54]. Since membranes with a PAH top layer are overall nearly uncharged, we assume that still some positive PAH moieties are available on the membrane surface. On the other side, PMPC-co-AA membranes are negatively charged, probably due to the residual AA groups.

Still, if the Donnan exclusion mechanism was the only mechanism responsible for ion retention, we would expect lower retentions of Ca^{2+}
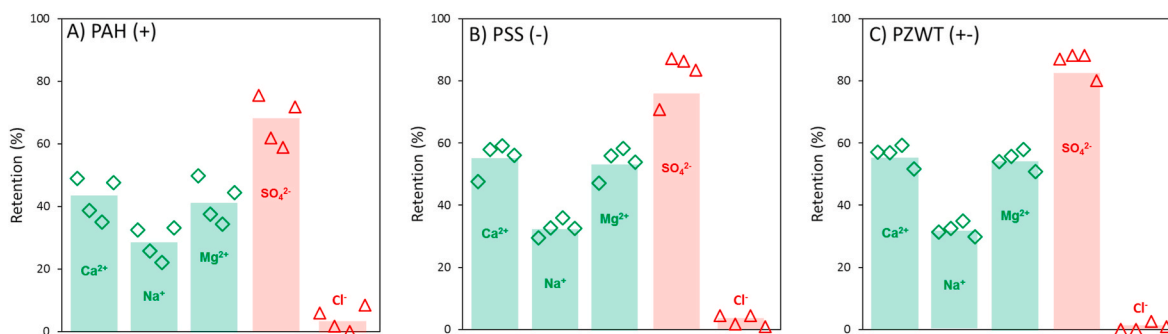
Fig. 3. Retentions of Ca^{2+}, Na^+, Mg^{2+}, SO_4^{2-} and Cl^- from membranes coated with A) PAH, B) PSS and C) PMPC-co-AA top layers in experiments performed with synthetic surface water. The synthetic surface water was made of 2.92 mM NaCl, 0.57 mM MgSO$_4$, 1.47 mM CaSO$_4$ and 0.3 mM MgCl$_2$[62]. Bars show average values, while markers show data points from all individual measurements.

and Mg^{2+} respect to Na^+. But other ions exclusion mechanisms, such as dielectric exclusion [81], can take place in our system. In particular, the dielectric exclusion mechanism may explain why Ca^{2+} and Mg^{2+} have a higher retention than Na^+. Ions and polymer moieties polarise their interfaces in water proportionally to their ionic charge. Differences in dielectric constants of the water between bulk solution and membrane separation layer contribute to an exclusion energy, which is proportional to the square of the ion charge [81], higher for divalent ions than monovalent ions [83]. This effect would thus be caused by the inner part of the polyelectrolyte multilayer, indeed leading to quite similar salt retentions for the three membranes where only the final outer layer is different.

3.2.2. Filtration of lysozyme

In Fig. 4, we show ion retentions and flux decline for crossflow filtration experiments carried out on synthetic surface water with positively charge Lysozyme as a model foulant. Specifically, Fig. 4A–C, show ion retentions, as well as lysozyme retention, and flux decline respectively for cationic PAH, anionic PSS and zwitterionic PMPC-co-AA terminated PEM based NF membranes. Flux recovery is discussed together with irreversibility of adsorption in the SI, Fig. S6.

For PAH (Fig. 4A) and PSS (Fig.4B) top layers, we do observe a significant increase in divalent cations retention (Ca^{2+} and Mg^{2+}) compared to Fig. 3A and B, respectively. Contrarily, no significant changes in retention are observed for PMPC-co-AA surface chemistry (Figs. 4C and 3C). In addition, Fig. 4A and B shows ~30% and ~45% flux decline, respectively for PAH and PSS top layers, while almost no flux decline is observed for PMPC-co-AA chemistry (Fig. 4C).

The flux decline observed for PAH and PSS, together with the increased retention in divalent cations, strongly suggest the build-up of a lysozyme fouling layer on top of the membrane surface. Lysozyme is completely retained by the membranes, and since they are positively charged, their adhesion to the membrane surface leads to an increase in Ca^{2+} and Mg^{2+} retention. This change in retention is mainly driven by additional Donnan exclusion effects. Sulphate, SO_4^{2-}, is, however, still highly retained by the membrane, proving that retention is the result of a combination of effects, dielectric exclusion [81] and electroneutrality included.

Lysozyme is positively charged around neutral pH [84] and its adsorption on negative surfaces is mainly driven by electrostatic forces [85]. On negative Silica, lysozyme adsorption changes the zeta potential from negative to positive values [86]. Previous studies have reported high degrees of adsorption and fouling on negatively charged NF and UF membranes [87]. However, lysozyme is a small protein, with a molecular weight of ~14.3 kDa [88]. Lysozyme due to its size cannot diffuse through the membrane and it is thus stopped at the membrane surface where adsorption takes place. Therefore the inner layers will still keep their negative charge.

While a flux decline is observed for PAH fouled by lysozyme, the observed adsorption values (Fig. 2) were rather low. This could indicate a more dominant role of foulant-foulant interactions in the observed fouling. In reflectometry experiments we do see a small lysozyme adsorption on PMPC-co-AA surfaces (Fig. 2C), but it does not influence the flux, probably due to the formation of a much more open fouling layer. The high degree of hydration of the zwitterionic moieties leads to a large energy barrier for the protein adsorption [49], preventing the build-up of a dense gel layer on top of the membrane.

3.2.3. Filtration of BSA

Fig. 5 shows the results of our crossflow filtration tests where BSA, as the model foulant, is added to our synthetic surface water. Here, Fig. 5A–C, show ion retentions, BSA retention and flux decline respectively for PAH, PSS and PMPC-co-AA top layers.

For PAH (Fig. 5A) and for PSS (Fig. 5B) surfaces, we mainly observe a small (~10%) increase in sulphate SO_4^{2-} retention compared to filtration without foulants (Fig. 3A and B). Contrarily, for our polyzwitterionic top
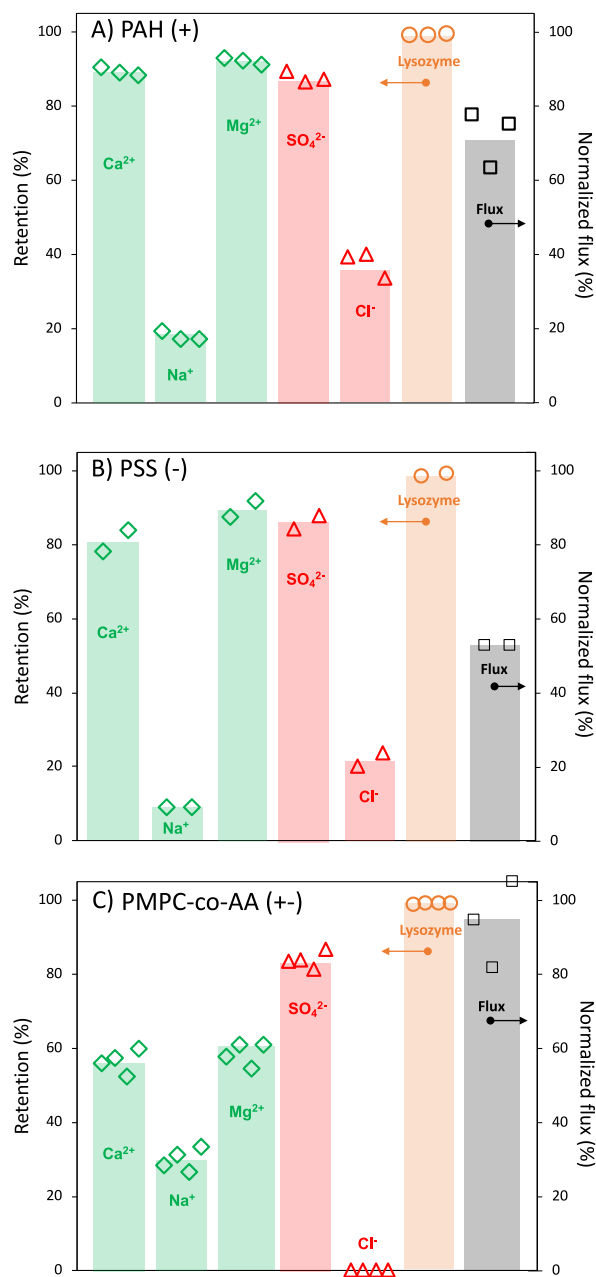
Fig. 4. Retentions of Ca^{2+}, Na^+, Mg^{2+}, SO_4^{2-}, Cl^-, Lysozyme and normalized flux (after fouling) for membranes coated with A) PAH, B) PSS and C) PMPC-co-AA top layers in experiments performed with synthetic surface water. The synthetic surface water was made of 2.92 mM NaCl, 0.57 mM MgSO$_4$, 1.47 mM CaSO$_4$, 0.3 mM MgCl$_2$ and 100 mg/L of Lysozyme. Bars show average values, while markers show data points from all individual measurements.

layer, made of PMPC-*co*-AA, we observe almost ~10% decrease in all divalent ions retention (see Figs. 5C and 3C). Again, PAH and PSS present flux decline (respectively ~20% and ~45%, see Fig. 5A and B), while no flux decline is observed for PMPC-co-AA surface chemistry (Fig. 5C).

The flux decline, observed for PAH and PSS, suggests that a BSA fouling layer maybe responsible for the increased retention in sulphate. BSA is a relatively big protein (66.5 kDa, bigger than lysozyme) and negatively charged at neutral pH [86]. Adsorption of BSA on PAH and PSS membranes can explain why SO_4^{2-} retention increases (increased Donnan exclusion). In addition, BSA is overall well retained by all our
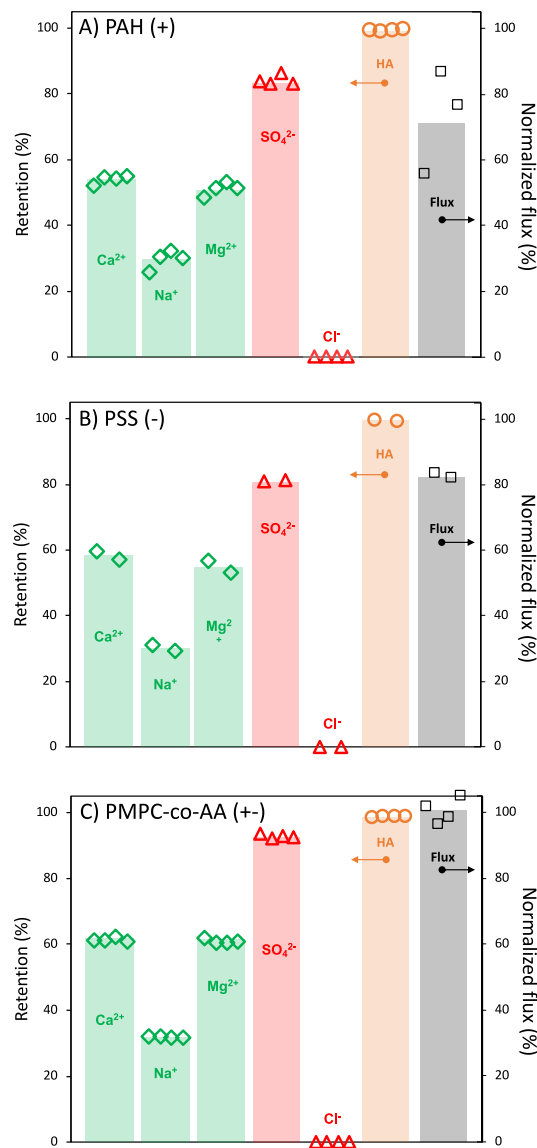
E. Virga et al.
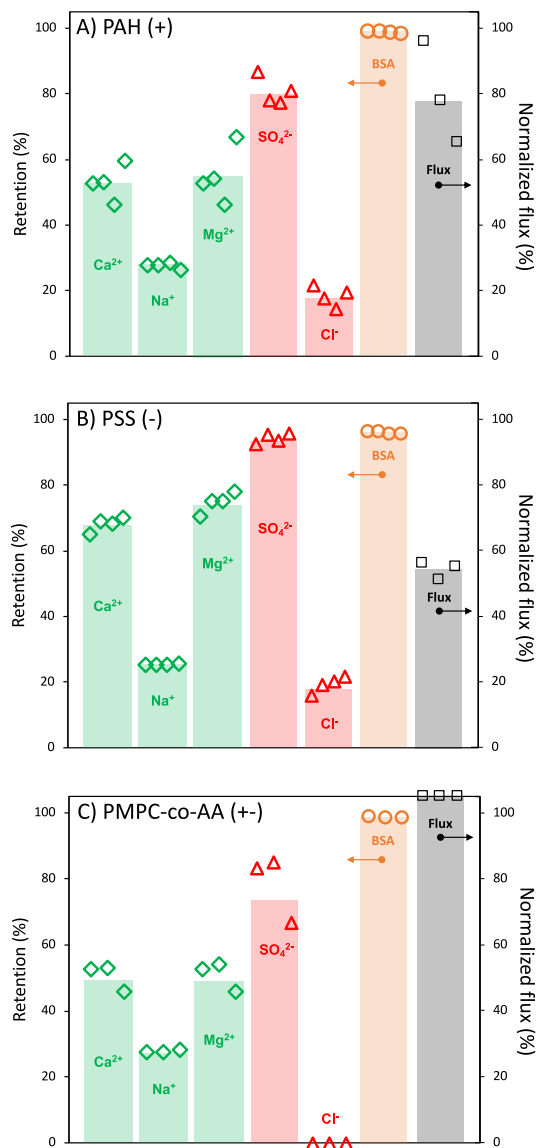
Fig. 5. Retentions of Ca^{2+}, Na^+, Mg^{2+}, SO_4^{2-}, Cl^-, BSA and normalized flux (after fouling) for membranes coated with A) PAH, B) PSS and C) PMPC-co-AA top layers in experiments performed with synthetic surface water. The synthetic surface water was made of 2.92 mM NaCl, 0.57 mM MgSO$_4$, 1.47 mM CaSO$_4$, 0.3 mM MgCl$_2$ and 100 mg/L of BSA. Bars show average values, while markers show data points from all individual measurements.

Fig. 6. Retentions of Ca^{2+}, Na^+, Mg^{2+}, SO_4^{2-}, Cl^-, HA and normalized flux (after fouling) for membranes coated with A) PAH, B) PSS and C) PMPC-co-AA top layers in experiments performed with synthetic surface water. The synthetic surface water was made of 2.92 mM NaCl, 0.57 mM MgSO$_4$, 1.47 mM CaSO$_4$, 0.3 mM MgCl$_2$ and 100 mg/L of HA. Bars show average values, while markers show data points from all individual measurements.

membranes.

Fig. 5 also shows that BSA fouls PSS membranes more strongly than PAH membranes. This result is in agreement with the adsorption studies we carried out on model surfaces (paragraph 3.1, Fig. 2). Indeed, BSA is a patchy protein, and at the pH of our experiments (~6.5) it has a small region with positive charge [77] which can complex with negatively charged PSS [33]. As discussed before, BSA may adsorb better, and therefore increase fouling, on PSS rather than PAH, due to charge regulation, that can lead to protein charge inversion [68].

3.2.4. Filtration of humic acids and alginates

In Fig. 6, we show the results obtained for Humic Acids as fouling agent. For PAH (Fig. 6A) and PMPC-co-AA (Fig. 6C) we observe ~10% increase in sulphate SO_4^{2-} retention compared to filtration without foulants (Fig. 3A). For membranes with PSS top layers, we have no significant changes in ion retentions (Fig. 6B). PAH shows ~25% flux

decline (Fig. 6A), PSS ~15% (Fig. 6B), but again no flux decline is observed for PMPC-co-AA (Fig. 6C).

The flux decline, observed for PAH, may suggest the build-up of a HA fouling layer which could increase the retention of sulphate. These HA are a mixture of negatively charged organic molecules, where the charge is mainly due to carboxyl groups [89]. Adsorption of HA on PAH may constitute a negatively charged layer on top which, via Donnan exclusion, increases the retention of SO_4^{2-}. This fouling layer does not clearly influence the retentions for PSS membranes. In addition, HA are ~100% retained by all our membranes.
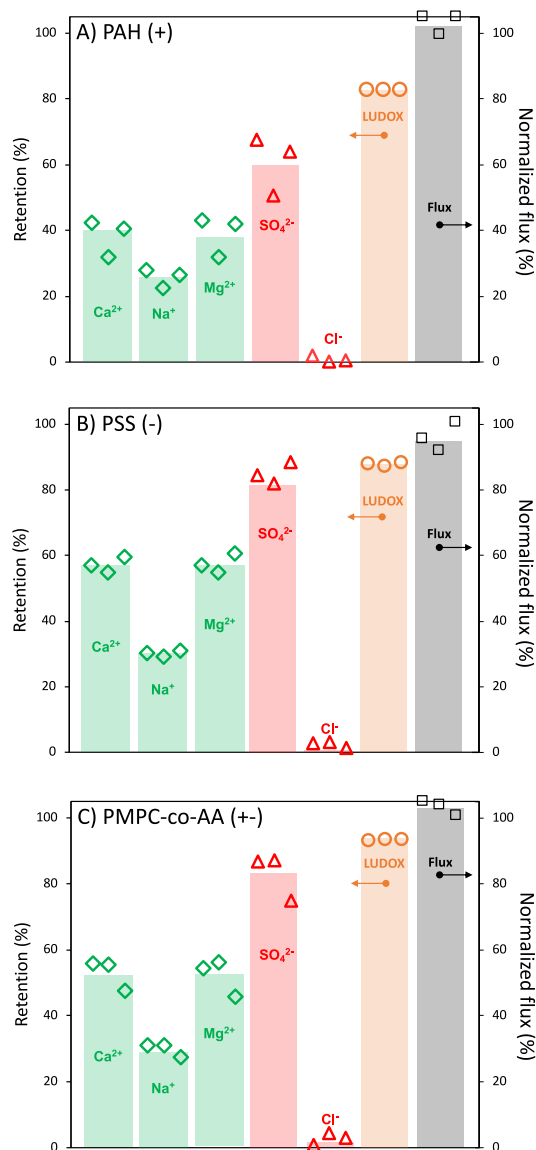
Very similar behaviour is observed for Alginates, for which we do not see significant differences in retention for PAH and PSS top layers, while we do note, in both cases, ~15% flux decline (SI, Fig. S7). For both HA and alginates with PSS we observed flux decline but little adsorption (Fig. 2). This may be due to foulant-foulant interactions which could dominate in the observed fouling. For PMPC-co-AA top layer, we

observe ~10% increase in sulphate retention, but no flux decline (Fig. S6).

Our alginates are acid polysaccharides present in the extracellular matrix of brown algae [90]. The alginate used in this study has a molecular weight distribution from about 12 to about 80 kDa and contains approximate 61% mannuronic acid and 39% guluronic acid [91]. The high carboxylate content gives rise to a high propensity to form cation-stabilized gels, especially with Mg^{2+} and Ca^{2+} [92]. Such a gel layer may cause flux decline in both PAH and PSS membranes. On the other hand, the 2-methacryloyloxyethyl phosphorylcholine (MPC) moiety of our PMPC-co-AA is believed to keep the free water fraction on the top layer surface at a high level [93], which may inhibit the polysaccharides adsorption.

3.2.5. Filtration of LUDOX colloidal silica

In Fig. 7, we show the results for LUDOX® colloidal silica. For LUDOX® particles, we do not observe significant differences in retention for all top layers (Fig. 8A–C)fig5. However, such a low retention is unexpected relatively to the size of colloidal size (12 nm). We can easily conclude that this result was probably affected by the dissolution of silicon from glassware the permeate analysis. In addition, almost no flux decline is monitored in all cases. This result is no surprise, as colloidal silica is negatively charged, as well as our membranes, and relatively big (12 nm in diameter) compared to the other model foulants. For this reason a dense fouling layer, on top of the membrane surface, is unlikely to be formed. However, in reflectometry we observed significant fouling for top layers, while in our filtration experiments no fouling was observed. Colloidal particles are known to give very open cake layers [94], therefore the resistance of the colloidal silica cake layer is quite low compared to the NF membrane resistance. This can explain why, even if there is expected to be adsorption, colloidal fouling does not significantly affect the NF flux or the separation performance.

3.3. Treatment of real surface water and stability of membranes performance

3.3.1. Real surface water treatment

A hollow fiber NF membrane with a low-fouling tendency would be highly beneficial for surface water treatment, as one could remove organics and multivalent ions from water at lower energy consumption.

In Fig. 8, we show ion (Ca^{2+}, Na^+, Mg^{2+}, SO_4^{2-}, Cl^-) and organics (TOC) retentions for HF membranes with different top layers (PAH, PSS and PMPC-co-AA, respectively Fig. 8A–C). The ion retentions of the three different top layers do not differ significantly from the experiments we carried out with synthetic surface water (Fig. 3). Differently, the three membranes present quite different retention values for organics, which do not reflect the experiments carried out with our model foulants. In particular, PAH presents a retention average of ~40%, PSS ~0% and PMPC-co-AA ~70%. No significant flux decline was observed in all three cases.

The similarities between Figs. 8 and 3, together with similarities in feeds concentrations, suggest that the retention is not affected by the presence of a fouling layer, which also explains why no flux decline was observed. Differently, organics are able to permeate through the membrane, suggesting that probably the organics in the feed have (in average) a relatively low molecular weight compared to the model foulants that we tested.
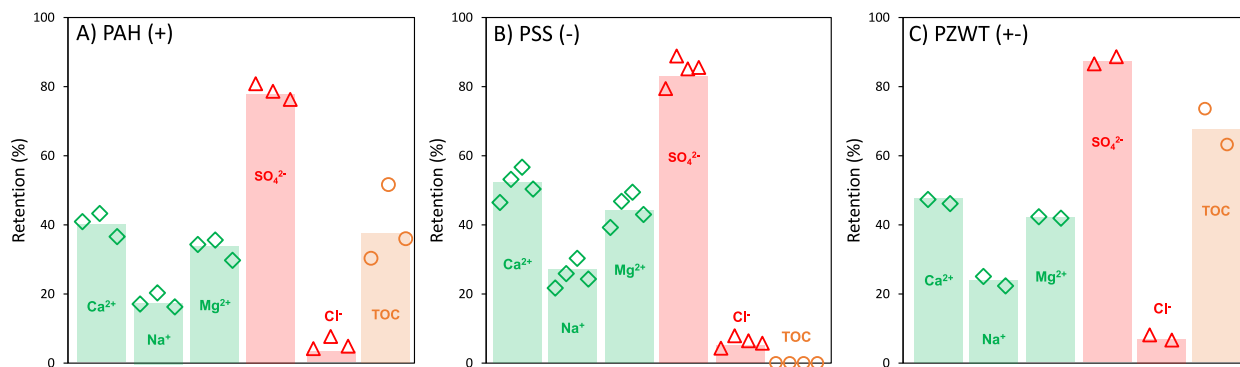
The relative organics retention is found to increase in the order PSS < PAH < PMPC-co-AA and can be a consequence of the relative water permeability which, inversely, decreases in the same order PSS > PAH > PMPC-co-AA (11.8, 7.8 and 5.45 LMH/bar, respectively, SI). Membranes terminated with PSS are more permeable to water than PAH membranes, probably due to their higher hydration [95]. On the other side, the PMPC-co-AA membrane is denser, probably due to the additional crosslinking of the carboxyl-amine groups [55,56]. We can conclude that our zwitterionic surface chemistry performed really well, since it did not exhibit fouling and additionally it retained 70% of the organics in the feed.

3.3.2. Overall performance stability

Fouling compromises the stability and selectivity of membrane separations [96], as it leads to an increase in hydraulic resistance during filtration, additional energetic costs, and frequent need for chemical cleaning [97]. All these factors lead to a productivity decline in water treatment, which is connected with the decline in permeability and the need to supply additional energy to keep filtration performances constant overtime.

For efficient industrial applications, membranes need to demonstrate stable performances overtime. A stable performance ideally translates into fouling resistant membranes, which ideally allow for a constant water permeability and stable permeate quality. Unfortunately, commercial membranes are usually charged, and as investigated in section

Fig. 7. Retentions of Ca^{2+}, Na^+, Mg^{2+}, SO_4^{2-}, Cl^-, LUDOX® and normalized flux (after fouling) for membranes coated with A) PAH, B) PSS and C) top layers in experiments performed with synthetic surface water. The synthetic surface water was made of 2.92 mM NaCl, 0.57 mM MgSO₄, 1.47 mM CaSO₄, 0.3 mM MgCl₂ and 100 mg/L of LUDOX®. Bars show average values, while markers show data points from all individual measurements.

Fig. 8. Retentions of Ca^{2+}, Na^+, Mg^{2+}, SO_4^{2-}, Cl^- and TOC from membranes coated with A) PAH, B) PSS and C) PMPC-co-AA top layers in experiments performed with real surface water collected at Afsluitdijk and pre-filtered with sand filter and cartridge filter. Bars show average values, while markers show data points from all individual measurements.

3.2, this charge excess can lead to fouling.

Collecting the results of the experiments shown in section 3.2, we studied the performance of our membranes in all our experiments and analyzed their stability. In Fig. 9, we show the stability of our membranes in terms of normalized flux (Fig. 9A) and deviation, Δ, in divalent ions retention (Fig. 9B), i.e. the percentage of deviation in Ca^{2+}, Mg^{2+} and SO_4^{2-} retention. This parameter is calculated for each ion by subtracting the retention of the divalent ion for a clean membrane from the actual retention, and then dividing the result by the clean membrane retention.

From Fig. 9, we can see how the membrane surface chemistry, the only difference between our membranes, plays a big role both in flux decline and retention properties compared to clean membranes. In Fig. 9A, we can see that while PAH and PSS top layered membranes show significant flux declines, the zwitterionic top layer allows for stable water fluxes, which is ideal from an industrial perspective. The high fouling resistance of our PMPC-co-AA membrane is mainly related to the preservation of the water structure at the membrane surface-solution interface. The high degree of hydration around the zwitterionic moieties, mainly due to strong electrostatic interactions and hydrogen bonding, leads to a large energy barrier which prevents the adsorption of foulants [49].

On the other side, Fig. 9B shows how fouling affects the retention properties of our membranes in terms of divalent ions retention. PAH, due to the formation of fouling layer, increases retention of divalent ions up to 120%, while for PSS the performances a more stable with highest changes around 70%. Again, the zwitterionic top layers allow for stable performances with way smaller changes in retention, which oscillate

around the zero value. This translates into a quality of the permeate constant overtime. We can conclude that, if we look at both parameters, our zwitterionic top layer is highly beneficial since it allows for stable water permeability and permeate quality during filtration, for all five model foulants. Still, future studies could focus on further optimizing the PMPC-co-AA membrane, in particular its water permeability.

During the last decades, thin film composite (TFC) membranes have been extensively used in RO [98] and NF processes [99]. The most commonly used TFC membranes (e.g. produced by Dow Filmtech and Hydronautics) [100] consist of an active polyamide layer deposited on a porous polysulfone support [82]. At neutral pH, TFC membranes have similar zeta potential to our crosslinked PAH membranes [101]. During chemical crosslinking, the primary amines ($pK_a \sim 9$) of our PAH layers convert into imines ($pK_a \sim 4$) giving, at neutral pH, a net negative charge to the membrane [82]. Our PAH terminated membranes thus have a comparable charge, crosslinked structure and a relatively similar chemical structure (imine bonds instead of amide) at the membrane surface as TFC membranes.

For the above reasons we do believe that the finding of our work, especially the results obtained for PAH membranes, are relevant for TFC membranes. Still, other determinant factors, such as membrane roughness and specific acid-base interactions, need to be considered. It is well known that a higher surface roughness, typically associated to TFC membranes, would increase the rate and extent of colloidal fouling [102], while stronger lewis acid-base interactions between membrane and foulant could also worsen membrane fouling.

An important point to make, however, is that polyamide TFC membranes are still commercially available only as flat sheets, as it is quite
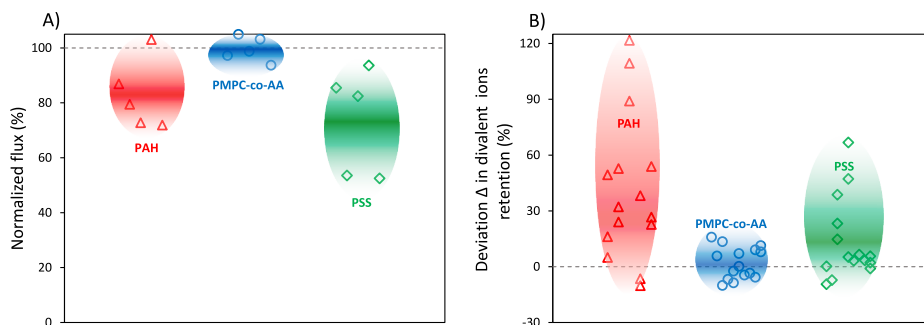
Fig. 9. Membranes performance, for PAH, PSS and PMPC-co-AA top layer, in terms of A) Normalized flux (%) and B) Deviation Δ in divalent ion retention (%). Markers represent the average of Figs.4–7 data points, while shapes enclosing these markers darken on the average for each top layer.

difficult to make TFC membranes via IP in a hollow fiber configuration [103]. Here, our PEM based membranes have the advantage that hollow fiber manufacturing is very straightforward. In regards to fouling, hollow fiber membranes have the large advantage compared to flat sheet (spiral wound) configurations that spacer fouling is not a problem.

4. Conclusions

Charged interfaces, usually present in commercial membranes, have the downside that fouling of oppositely charged components can readily occur. This can increase filtration costs and affect separation selectivity. In this work, we investigated the effect of membranes surface chemistry on fouling during surface water treatment for polyelectrolyte multilayer based nanofiltration membranes. We prepared three membranes with the same active separation layer but a different surface chemistry, including nearly uncharged crosslinked PAH, strongly negatively charged PSS and zwitterionic PMPC-co-AA. Initially, we focused on foulant adsorption for the three differently terminated multilayers on model surfaces to demonstrate how a different surface chemistry of the top layer affects the subsequent adsorption of five different model foulants (Humic Acids, Alginates, Silica Nanoparticles, negatively and positively charged Proteins). Later, we studied fouling of the same model foulants on our polyelectrolyte multilayer based hollow fiber NF membranes with identical surface chemistries to the model surfaces. Generally, the nearly uncharged crosslinked PAH surface chemistry fouls more than the strongly negatively charged PSS. While negative BSA adsorbs better on PSS, probably due to charge regulation. Overall fouling was mainly driven by electrostatic and acid-base interactions, which led, for both nearly uncharged crosslinked PAH and strongly negatively PSS, to flux decline and changes in separation selectivity. Filtration experiments, carried out with synthetic and real surface water, demonstrated that our bio-inspired zwitterionic phosphatidylcholine surface chemistry exhibits excellent fouling resistance and stable performances during filtration. The stable selectivity, and exceptional fouling resistance of these membranes makes them promising not only for surface water treatment but also for bio-molecule separation, and filtration of other feeds with large fouling potential.

CRediT authorship contribution statement

Ettore Virga: Conceptualization, Data curation, Investigation, Methodology, Writing - original draft. **Klara Žvab:** Data curation, Investigation, Writing - review & editing. **Wiebe M. de Vos:** Conceptualization, Project administration, Supervision, Writing - review & editing, Funding acquisition.

Declaration of competing interest

The authors declare that they have no known competing financial interests or personal relationships that could have appeared to influence the work reported in this paper.

Acknowledgement

Appendix A. Supplementary data

Supplementary data to this article can be found online at https://doi.org/10.1016/j.memsci.2020.118793.

References

[1] B. Van Der Bruggen, C. Vandecasteele, T. Van Gestel, W. Doyen, R. Leysen, A review of pressure-driven membrane processes in wastewater treatment and drinking water production, Environ. Prog. 22 (2003) 46–56.

[2] D.M. Warsinger, et al., A review of polymeric membranes and processes for potable water reuse, Prog. Polym. Sci. 81 (2018) 209–237.

[3] A. Mohammad, Y. Teow, W. Ang, Y. Chung, D. Oatley-Radcliffe, N. Hilal, Nanofiltration membranes review: recent advances and future prospects, Desalination 356 (2015) 226–254 (State-of-the-Art Reviews in Desalination).

[4] A.R. Costa, M.N. de Pinho, Performance and cost estimation of nanofiltration for surface water treatment in drinking water production, Desalination 196 (2006) 55–65.

[5] R. Bian, Y. Watanabe, N. Tambo, G. Ozawa, Removal of humic substances by UF and NF membrane systems, Water Sci. Technol. 40 (1999) 121–129.

[6] D.M. Reurink, E. te Brinke, I. Achterhuis, H.D.W. Roesink, W.M. de Vos, Nafion-based low-hydration polyelectrolyte multilayer membranes for enhanced water purification, ACS Applied Polymer Materials 1 (2019) 2543–2551.

[7] K.V. Plakas, A.J. Karabelas, Removal of pesticides from water by NF and RO membranes — a review, Desalination 287 (2012) 255–265. Special Issue in honour of Professor Takeshi Matsuura on his 75th Birthday.

[8] M. Pontié, C. Diawara, M. Rumeau, D. Aureau, P. Hemmery, Seawater nanofiltration (NF): fiction or reality? Desalination 158 (2003) 277–280 (Desalination and the Environment: Fresh Water for All).

[9] L. Naidu, S. Saravanan, C. Manickam, M. Goel, A. Das, J. Babu, Nanofiltration in transforming surface water into healthy water: comparison with reverse osmosis, J. Chem. (2015) 1–6, 2015.

[10] W. Guo, H.-H. Ngo, J. Li, A mini-review on membrane fouling, Bioresour. Technol. 122 (2012) 27–34. Membrane Bioreactors (MBRs): State-of-Art and Future.

[11] W. Zhang, B. Dong, Effects of physical and chemical aspects on membrane fouling and cleaning using interfacial free energy analysis in forward osmosis, Environ. Sci. Pollut. Control Ser. 25 (2018) 21555–21567.

[12] N. Porcelli, S. Judd, Chemical cleaning of potable water membranes: a review, Separ. Purif. Technol. 71 (2010) 137–143.

[13] X. Shi, G. Tal, N.P. Hankins, V. Gitis, Fouling and cleaning of ultrafiltration membranes: a review, J. Water Process Eng. 1 (2014) 121–138.

[14] C. Bellona, M. Marts, J.E. Drewes, The effect of organic membrane fouling on the properties and rejection characteristics of nanofiltration membranes, Separ. Purif. Technol. 74 (2010) 44–54.

[15] F. Kramer, R. Shang, L. Rietveld, S. Heijman, Influence of pH, multivalent counter ions, and membrane fouling on phosphate retention during ceramic nanofiltration, Separ. Purif. Technol. 227 (2019) 115675.

[16] Y. ying Zhao, X. mao Wang, H. wei Yang, F. feng, Y. Xie, Effects of organic fouling and cleaning on the retention of pharmaceutically active compounds by ceramic nanofiltration membranes, J. Membr. Sci. 563 (2018) 734–742.

[17] L.D. Nghiem, S. Hawkes, Effects of membrane fouling on the nanofiltration of pharmaceutically active compounds (PhACs): mechanisms and role of membrane pore size, Separ. Purif. Technol. 57 (2007) 176–184.

[18] B. Van der Bruggen, M. Mänttäri, M. Nyström, Drawbacks of applying nanofiltration and how to avoid them: a review, Separ. Purif. Technol. 63 (2008) 251–263.

[19] M.F.A. Goosen, S.S. Sablani, H. Al-Hinai, S. Al-Obeidani, R. Al-Belushi, D. Jackson, Fouling of reverse osmosis and ultrafiltration membranes: a critical review, Separ. Sci. Technol. 39 (2005) 2261–2297.

[20] I. Ibrar, O. Naji, A. Sharif, A. Malekizadeh, A. Al Hawari, A. Alhathal Alanezi, A. Altaee, A review of fouling mechanisms, control strategies and real-time fouling monitoring techniques in forward osmosis, Water 11 (2019) 695.

[21] R. Oliveira, Understanding adhesion: a means for preventing fouling, Exp. Therm. Fluid Sci. 14 (1997) 316–322.

[22] B. He, Y. Ding, J. Wang, Z. Yao, W. Qing, Y. Zhang, F. Liu, C.Y. Tang, Sustaining fouling resistant membranes: membrane fabrication, characterization and mechanism understanding of demulsification and fouling-resistance, J. Membr. Sci. 581 (2019) 105–113.

[23] D. Norberg, S. Hong, J. Taylor, Y. Zhao, Surface characterization and performance evaluation of commercial fouling resistant low-pressure RO membranes, Desalination 202 (2007) 45–52 (Wastewater Reclamation and Reuse for Sustainability).

[24] L. Upadhyaya, X. Qian, S.R. Wickramasinghe, Chemical modification of membrane surface—overview, Current Opinion in Chemical Engineering 20 (2018) 13–18 (Nanotechnology/Separation Engineering).

[25] Y.-R. Chang, Y.-J. Lee, D.-J. Lee, Membrane fouling during water or wastewater treatments: current research updated, J. Taiwan Institute of Chem. Eng. 94 (2019) 88–96.

[26] G.-d. Kang, Y.-m. Cao, Development of antifouling reverse osmosis membranes for water treatment: a review, Water Res. 46 (2011) 584–600.

[27] S.M.J. Zaidi, K.A. Mauritz, M.K. Hassan, in: M.A. Jafar Mazumder, H. Sheardown, A. Al-Ahmed (Eds.), In Functional Polymers, Springer International Publishing, Cham, 2019, pp. 391–416.

[28] S.P. Nunes, Can fouling in membranes be ever defeated? Current Opinion in Chemical Engineering 28 (2020) 90–95.

[29] J. Saqib, I.H. Aljundi, Membrane fouling and modification using surface treatment and layer-by-layer assembly of polyelectrolytes: state-of-the-art review, J. Water Process Eng. 11 (2016) 68–87.

[30] F. Crespilho, V. Zucolotto, O. Oliveira, Electrochemistry of layer-by-layer films: a review, Int. J. Electrochemical Sci. 1 (2006).

[31] W. Jin, A. Toutianoush, B. Tieke, Use of polyelectrolyte layer-by-layer assemblies as nanofiltration and reverse osmosis membranes, Langmuir 19 (2003) 2550–2553.

[32] V.A. Izumrudov, B.K. Mussabayeva, K.B. Murzagulova, Polyelectrolyte multilayers: preparation and applications, Russ. Chem. Rev. 87 (2018) 192–200.

[33] W.M. de Vos, S. Lindhoud, Overcharging and charge inversion: finding the correct explanation(s), Adv. Colloid Interface Sci. 274 (2019) 102040.

[34] L.Y. Ng, A.W. Mohammad, C.Y. Ng, A review on nanofiltration membrane fabrication and modification using polyelectrolytes: effective ways to develop membrane selective barriers and rejection capability, Adv. Colloid Interface Sci. 197–198 (2013) 85–107.

[35] N. Joseph, P. Ahmadiannamini, R. Hoogenboom, I.F.J. Vankelecom, Layer-by-layer preparation of polyelectrolyte multilayer membranes for separation, Polym. Chem. 5 (2014) 1817–1831.

[36] J. de Grooth, R. Oborný, J. Potreck, K. Nijmeijer, W.M. de Vos, The role of ionic strength and odd–even effects on the properties of polyelectrolyte multilayer nanofiltration membranes, J. Membr. Sci. 475 (2015) 311–319.

[37] D. Menne, J. Kamp, J.E. Wong, M. Wessling, Precise tuning of salt retention of backwashable polyelectrolyte multilayer hollow fiber nanofiltration membranes, J. Membr. Sci. 499 (2016) 396–405.

[38] J.J. Harris, J.L. Stair, M.L. Bruening, Layered polyelectrolyte films as selective, ultrathin barriers for anion transport, Chem. Mater. 12 (2000) 1941–1946.

[39] M.L. Bruening, D.M. Sullivan, Enhancing the ion-transport selectivity of multilayer polyelectrolyte membranes, Chem. Eur J. 8 (2002) 3832–3837.

[40] C. Ba, D.A. Ladner, J. Economy, Using polyelectrolyte coatings to improve fouling resistance of a positively charged nanofiltration membrane, J. Membr. Sci. 347 (2010) 250–259.

[41] T. Ishigami, K. Amano, A. Fujii, Y. Ohmukai, E. Kamio, T. Maruyama, H. Matsuyama, Fouling reduction of reverse osmosis membrane by surface modification via layer-by-layer assembly, Separ. Purif. Technol. 99 (2012) 1–7.

[42] F. Fadhillah, A.M. Alghamdi, M.D. Alsubei, S.A. Aljlil, Synthesis of protein-fouling-resistance polyelectrolyte multilayered nanofiltration membranes through spin-assisted layer-by-layer assembly, J. King Saud University - Eng. Sci. (2020), https://doi.org/10.1016/j.jksues.2020.04.003.

[43] D.M. Reurink, J.P. Haven, I. Achterhuis, S. Lindhoud, E.H.D.W. Roesink, W.M. de Vos, Annealing of polyelectrolyte multilayers for control over ion permeation, Adv. Mat. Interfaces 5 (2018) 1800651.

[44] R.W. Baker, Membrane Technology and Applications, Chapter 6, John Wiley & Sons, Ltd, 2012, pp. 253–302.

[45] M. Hadidi, A.L. Zydney, Fouling behavior of zwitterionic membranes: impact of electrostatic and hydrophobic interactions, J. Membr. Sci. 452 (2014) 97–103.

[46] J. B. Zwitteration Schlenoff, Coating surfaces with zwitterionic functionality to reduce nonspecific adsorption, Langmuir 30 (2014) 9625–9636. PMID: 24754399.

[47] M. He, K. Gao, L. Zhou, Z. Jiao, M. Wu, J. Cao, X. You, Z. Cai, Y. Su, Z. Jiang, Zwitterionic materials for antifouling membrane surface construction, Acta Biomater. 40 (2016) 142–152. Zwitterionic Materials.

[48] P. Bengani, Y. Kou, A. Asatekin, Zwitterionic copolymer self-assembly for fouling resistant, high flux membranes with size-based small molecule selectivity, J. Membr. Sci. 493 (2015) 755–765.

[49] P. Bengani-Lutz, E. Converse, P. Cebe, A. Asatekin, Self-assembling zwitterionic copolymers as membrane selective layers with excellent fouling resistance: effect of zwitterion chemistry, ACS Appl. Mater. Interfaces 9 (2017) 20859–20872. PMID: 28544845.

[50] M. Singh, N. Tarannum, In engineering of biomaterials for drug delivery systems, in: A. Parambath (Ed.), Woodhead Publishing Series in Biomaterials, Woodhead Publishing, 2018, pp. 69–101.

[51] J.B. Schlenoff, H. Ly, M. Li, Charge and mass balance in polyelectrolyte multilayers, J. Am. Chem. Soc. 120 (1998) 7626–7634.

[52] P. Lavalle, C. Picart, J. Mutterer, C. Gergely, H. Reiss, J.-C. Voegel, B. Senger, P. Schaaf, Modeling the buildup of polyelectrolyte multilayer films having exponential growth, J. Phys. Chem. B 108 (2004) 635–648.

[53] J. de Grooth, M. Dong, W.M. de Vos, K. Nijmeijer, Building polyzwitterion-based multilayers for responsive membranes, Langmuir 30 (2014) 5152–5161. PMID: 24749944.

[54] E. Virga, J. de Grooth, K. Žvab, W.M. de Vos, Stable polyelectrolyte multilayer-based hollow fiber nanofiltration membranes for produced water treatment, ACS Applied Polymer Materials 1 (2019) 2230–2239.

[55] K. Nam, T. Kimura, A. Kishida, Controlling coupling reaction of EDC and NHS for preparation of collagen gels using ethanol/water Co-solvents, Macromol. Biosci. 8 (2008) 32–37.

[56] M.J.E. Fischer, in: N.J. Mol, M.J.E. Fischer (Eds.), In Surface Plasmon Resonance: Methods and Protocols, Humana Press, Totowa, NJ, 2010, pp. 55–73.

[57] A. Nguyen, S. Azari, L. Zou, Coating zwitterionic amino acid l-DOPA to increase fouling resistance of forward osmosis membrane, Desalination 312 (2013) 82–87 (Recent Advances in Forward Osmosis).

[58] J. Dijt, M. Stuart, G. Fleer, Reflectometry as a tool for adsorption studies, Adv. Colloid Interface Sci. 50 (1994) 79–101.

[59] A. Theisen, Refractive Increment Data Book for Polymer and Biomolecular Scientists, Nottingham University Press, 2000.

[60] G. Deželić, J.P. Kratohvil, Determination of size of small particles by light scattering. experiments on ludox colloidal silica, Kolloid Z. 173 (1960) 38–48.

[61] A. Vermeer, Interactions between Humic Acid and Hematite and Their Effects on Metal Ion Speciation, 1996. Ph.D. thesis, WUR.

[62] T. Rijnaarts, J. Moreno, M. Saakes, W. Vos, K. Nijmeijer, Role of anion exchange membrane fouling in reverse electrodialysis using natural feed waters, Colloid. Surface. Physicochem. Eng. Aspect. (2018) 560.

[63] S.-H. Yoon, C.-H. Lee, K.-J. Kim, A.G. Fane, Effect of calcium ion on the fouling of nanofilter by humic acid in drinking water production, Water Res. 32 (1998) 2180–2186.

[64] C.Y. Tang, Y.-N. Kwon, J.O. Leckie, Fouling of reverse osmosis and nanofiltration membranes by humic acid—effects of solution composition and hydrodynamic conditions, J. Membr. Sci. 290 (2007) 86–94.

[65] W.-Y. Ahn, A.G. Kalinichev, M.M. Clark, Effects of background cations on the fouling of polyethersulfone membranes by natural organic matter: experimental and molecular modeling study, J. Membr. Sci. 309 (2008) 128–140.

[66] H. Shirahama, J. Lyklema, W. Norde, Comparative protein adsorption in model systems, J. Colloid Interface Sci. 139 (1990) 177–187.

[67] W. Norde, T. Arai, H. Shirahama, Protein adsorption in model systems, Biofouling 4 (1991) 37–51.

[68] W. de Vos, M. Biesheuvel, A. Keizer, M. Kleijn, M. Cohen Stuart, Adsorption of the protein bovine serum albumin in a planar poly(acrylic acid) brush layer as measured by optical reflectometry, Langmuir 24 (2008) 6575–6584.

[69] S. Ilyas, R. English, P. Aimar, J.-F. Lahitte, W.M. de Vos, Preparation of multifunctional hollow fiber nanofiltration membranes by dynamic assembly of weak polyelectrolyte multilayers, Colloid. Surface. Physicochem. Eng. Aspect. 533 (2017) 286–295.

[70] D. Xu, C. Hodges, Y. Ding, S. Biggs, A. Brooker, D. York, Adsorption kinetics of laponite and ludox silica nanoparticles onto a deposited poly (diallyldimethylammonium chloride) layer measured by a quartz crystal microbalance and optical reflectometry, Langmuir 26 (2010) 18105–18112. PMID: 21073154.

[71] P. van den Brink, A. Zwijnenburg, G. Smith, H. Temmink, M. van Loosdrecht, Effect of free calcium concentration and ionic strength on alginate fouling in cross-flow membrane filtration, J. Membr. Sci. 345 (2009) 207–216.

[72] H. Yamamura, K. Okimoto, K. Kimura, Y. Watanabe, Influence of calcium on the evolution of irreversible fouling in microfiltration/ultrafiltration membranes, J. Water Supply Res. Technol. - Aqua 56 (2007) 425–434.

[73] D. Zhao, S. Yu, A review of recent advance in fouling mitigation of NF/RO membranes in water treatment: pretreatment, membrane modification, and chemical cleaning, Desalination and Water Treatment 55 (2015) 870–891.

[74] R. Kumar, A.F. Ismail, Fouling control on microfiltration/ultrafiltration membranes: effects of morphology, hydrophilicity, and charge, J. Appl. Polym. Sci. 132 (2015).

[75] X. Jin, X. Huang, E.M. Hoek, Role of specific ion interactions in seawater RO membrane fouling by alginic acid, Environ. Sci. Technol. 43 (2009) 3580–3587. PMID: 19544858.

[76] C.J. van Oss, Interfacial Forces in Aqueous Media, Marcel Dekker, New York, 1994.

[77] E. Seyrek, P.L. Dubin, C. Tribet, E.A. Gamble, Ionic strength dependence of protein-polyelectrolyte interactions, Biomacromolecules 4 (2003) 273–282. PMID: 12625722.

[78] V.V. Murashov, J. Leszczynski, Adsorption of the phosphate groups on silica hydroxyls: an ab initio study, J. Phys. Chem. 103 (1999) 1228–1238.

[79] B. Mi, M. Elimelech, Chemical and physical aspects of organic fouling of forward osmosis membranes, J. Membr. Sci. 320 (2008) 292–302.

[80] H. Xu, K. Xiao, X. Wang, S. Liang, C. Wei, X. Wen, X. Huang, Outlining the roles of membrane-foulant and foulant-foulant interactions in organic fouling during microfiltration and ultrafiltration: a mini-review, Frontiers in Chemistry 8 (2020) 417.

[81] A.E. Yaroshchuk, Non-steric mechanisms of nanofiltration: superposition of Donnan and dielectric exclusion, Separ. Purif. Technol. 22–23 (2001) 143–158.

[82] K.L. Cho, A.J. Hill, F. Caruso, S.E. Kentish, Chlorine resistant glutaraldehyde crosslinked polyelectrolyte multilayer membranes for desalination, Adv. Mater. 27 (2015) 2791–2796.

[83] S. Bandini, D. Vezzani, Nanofiltration modeling: the role of dielectric exclusion in membrane characterization, Chem. Eng. Sci. 58 (2003) 3303–3326.

[84] Y.-N. Wang, C.Y. Tang, Nanofiltration membrane fouling by oppositely charged macromolecules: investigation on flux behavior, foulant mass deposition, and solute rejection, Environ. Sci. Technol. 45 (2011) 8941–8947. PMID: 21928796.

[85] K. Kubiak-Ossowska, P.A. Mulheran, Mechanism of hen egg white lysozyme adsorption on a charged solid surface, Langmuir 26 (2010) 15954–15965. PMID: 20873744.

[86] K. Rezwan, L. Meier, L. Gauckler, Lysozyme and bovine serum albumin adsorption on uncoated silica and AlOOH-coated silica particles: the influence of positively and negatively charged oxide surface coatings, Biomaterials 26 (2005) 4351–4357.

[87] Y. Wang, C. Tang, Fouling of nanofiltration, reverse osmosis, and ultrafiltration membranes by protein mixtures: the role of inter-foulant-species interaction, Environ. Sci. Technol. 45 (2011) 6373–6379.

[88] W. Burton, K. Nugent, T. Slattery, B. Summers, L. Snyder, Separation of proteins by reversed-phase high-performance liquid chromatography: I. Optimizing the column, J. Chromatogr. A 443 (1988) 363–379 (Seventh international symposium on high-performance liquid).

[89] J.D. Ritchie, E. Perdue, Proton-binding study of standard and reference fulvic acids, humic acids, and natural organic matter, Geochem. Cosmochim. Acta 67 (2003) 85–96.

[90] K. Queiroz, V. Medeiros, L. Queiroz, L. Abreu, H. Rocha, C. Ferreira, M. Jucá, H. Aoyama, E. Leite, Inhibition of reverse transcriptase activity of HIV by polysaccharides of brown algae, Biomed. Pharmacother. 62 (2008) 303–307.

[91] K.L. Chen, S.E. Mylon, M. Elimelech, Enhanced aggregation of alginate-coated iron oxide (hematite) nanoparticles in the presence of calcium, strontium, and barium cations, Langmuir 23 (2007) 5920–5928. PMID: 17469860.

[92] X. Jin, X. Huang, E.M. Hoek, Role of specific ion interactions in seawater RO membrane fouling by alginic acid, Environ. Sci. Technol. 43 (2009) 3580–3587. PMID: 19544858.

[93] K. Ishihara, H. Nomura, T. Mihara, K. Kurita, Y. Iwasaki, N. Nakabayashi, Why do phospholipid polymers reduce protein adsorption? J. Biomed. Mater. Res. 39 (1998) 323–330.

[94] K.W. Trzaskus, W.M. de Vos, A. Kemperman, K. Nijmeijer, Towards controlled fouling and rejection in dead-end microfiltration of nanoparticles – role of electrostatic interactions, J. Membr. Sci. 496 (2015) 174–184.

[95] J.E. Wong, F. Rehfeldt, P. Hänni, M. Tanaka, R.v. Klitzing, Swelling behavior of polyelectrolyte multilayers in saturated water vapor, Macromolecules 37 (2004) 7285–7289.

[96] R. Fabris, E.K. Lee, C.W. Chow, V. Chen, M. Drikas, Pre-treatments to reduce fouling of low pressure micro-filtration (MF) membranes, J. Membr. Sci. 289 (2007) 231–240.

[97] A. Zularisam, A. Ismail, R. Salim, Behaviours of natural organic matter in membrane filtration for surface water treatment — a review, Desalination 194 (2006) 211–231.

[98] G.-R. Xu, J.-M. Xu, H.-J. Feng, H.-L. Zhao, S.-B. Wu, Tailoring structures and performance of polyamide thin film composite (PA-TFC) desalination membranes via sublayers adjustment-a review, Desalination 417 (2017) 19–35.

[99] W. Lau, S. Gray, T. Matsuura, D. Emadzadeh, J. Paul Chen, A. Ismail, A review on polyamide thin film nanocomposite (TFN) membranes: history, applications, challenges and approaches, Water Res. 80 (2015) 306–324.

[100] J.M. Gohil, P. Ray, A review on semi-aromatic polyamide TFC membranes prepared by interfacial polymerization: potential for water treatment and desalination, Separ. Purif. Technol. 181 (2017) 159–182.

[101] G. Hurwitz, G.R. Guillen, E.M. Hoek, Probing polyamide membrane surface charge, zeta potential, wettability, and hydrophilicity with contact angle measurements, J. Membr. Sci. 349 (2010) 349–357.

[102] E.M. Vrijenhoek, S. Hong, M. Elimelech, Influence of membrane surface properties on initial rate of colloidal fouling of reverse osmosis and nanofiltration membranes, J. Membr. Sci. 188 (2001) 115–128.

[103] W. Lau, A. Ismail, N. Misdan, M. Kassim, A recent progress in thin film composite membrane: a review, Desalination 287 (2012) 190–199. Special Issue in honour of Professor Takeshi Matsuura on his 75th Birthday.